Sharp Transition for Single Polarons in the One-Dimensional Su-Schrieffer-Heeger Model

Sharp transition for single polarons in the one-dimensional Su-Schrieffer-Heeger model

D. J. J. Marchand[1], G. De Filippis[2], V. Cataudella[2], M. Berciu[1],
N. Nagaosa[3,5], N. V. Prokof'ev[4,6], A. S. Mishchenko[5,6], and P. C. E. Stamp[1]
[1] *Department of Physics and Astronomy, University of British Columbia, Vancouver, BC, Canada, V6T 1Z1*
[2] *CNR-SPIN and Dip. di Scienze Fisiche - Università di Napoli Federico II - I-80126 Napoli, Italy*
[3] *Department of Applied Physics, The University of Tokyo, 7-3-1 Hongo, Bunkyo-ku, Tokyo 113, Japan*
[4] *Department of Physics, University of Massachusetts, Amherst, Massachusetts 01003, USA*
[5] *Cross-Correlated Materials Research Group (CMRG), ASI, RIKEN, Wako 351-0198, Japan*
[6] *RRC "Kurchatov Institute" - 123182 - Moscow - Russia*

We study a single polaron in the Su-Schrieffer-Heeger (SSH) model using four different techniques (three numerical and one analytical). Polarons show a smooth crossover from weak to strong coupling, as a function of the electron-phonon coupling strength λ, in all models where this coupling depends only on phonon momentum q. In the SSH model the coupling also depends on the electron momentum k; we find it has a sharp transition, at a critical coupling strength λ_c, between states with zero and nonzero momentum of the ground state. All other properties of the polaron are also singular at $\lambda = \lambda_c$. This result is representative of all polarons with coupling depending on k and q, and will have important experimental consequences (eg., in ARPES and conductivity experiments).

PACS numbers: 72.10.-d, 71.10.Fd, 71.38.-k

Polarons have been of broad interest in physics ever since they were introduced in 1933, to describe dielectric charge carriers [1]. Apart from their central role in solid-state physics, with many models now in use [2–4], they exemplify in quantum field theory the passage from weak to strong coupling in a non-trivial model of a single particle coupled to a bosonic field [5]. The first serious non-perturbative studies by Feynman [6] of the Frohlich polaron, are now a classic, but only recently were accurate results established across the whole range of coupling strengths [7]. Since then, exact numerical studies have been made of, eg., D-dimensional Holstein polarons in various lattice geometries, with $D = 1, 2, 3$ [8]; of 3D Rashba-Pekar polarons with short-range interactions [9]; of pseudo Jahn-Teller polarons [10]; and so on.

A central question in this field has been whether a sharp transition can exist in the polaronic ground state as a function of the dimensionless effective particle-boson coupling λ. In all the above-cited work there is simply a smooth crossover, expected when the coupling depends only on the bosonic momentum q; then there must always be non-zero matrix elements between the ground state and excited polaron states [11]. However, quite generally, one expects the coupling to depend on both q and the particle momentum k; and then much less is known.

In this paper we study a specific example of this general case. The particle-boson coupling is taken from the well-known "SSH model", introduced to describe electrons in 1-d polyacetylene [12]. Here we focus on the single polaron limit, not the more common case of half-filling, and the bosons are chosen to describe optical phonons. While this ignores the acoustic phonons which exist in real materials, it allows a direct comparison with the large number of results known for models which have a purely q-dependent coupling. The Hamiltonian thus takes the simple form $\mathcal{H} = H_o + V + H_{ph}$, where

$$H_o = -t_o \sum_i (c_i^\dagger c_{i+1} + h.c.) \;\equiv\; \sum_k \epsilon_k c_k^\dagger c_k \;, \qquad (1)$$

describes the hopping of electrons between sites, with band dispersion $\epsilon_k = -2t_o \cos(k)$ ($c_i^\dagger$ creates an electron on site i; $c_k^\dagger$ creates a momentum state k). The term $H_{ph} = \omega_{ph} \sum_i b_i^\dagger b_i$ describes dispersionless phonons ($b_i^\dagger$ creates a phonon on site i). The interaction is

$$\begin{aligned} V &= -\tilde{\alpha} t_o \sum_i (\hat{X}_i - \hat{X}_{i+1})(c_i^\dagger c_{i+1} + h.c.) \\ &= N^{-1/2} \sum_{k,q} M(k,q) c_{k+q}^\dagger c_k (b_{-q}^\dagger + b_q) \end{aligned} \qquad (2)$$

with site displacements $\hat{X}_i = \sqrt{\frac{\hbar}{2M\omega_{ph}}} \left(b_i + b_i^\dagger\right)$, and an interaction vertex

$$\begin{aligned} M(k,q) &= 2i\alpha[\sin(k+q) - \sin(k)] \\ &= i(2\lambda\omega_{ph} t_o)^{1/2} [\sin(k+q) - \sin(k)] \end{aligned} \qquad (3)$$

This interaction, with associated energy $\alpha = \tilde{\alpha} t_o \sqrt{\frac{\hbar}{2M\omega_{ph}}}$, describes the modulation of the hopping amplitude by phonons. We henceforth set $t_o = 1$, and define two dimensionless parameters: the electron-phonon coupling parameter $\lambda = 2\alpha^2/(t_o\omega_{ph}) = \langle |M(k,q)|^2 \rangle / (2t_o\omega_{ph})$, where $\langle\cdot\rangle$ averages over the Brillouin zone; and the 'adiabaticity' ratio ω_{ph}/t_o ($\equiv \omega_{ph}$ when $t_o = 1$).

(i) Results: We treat this non-perturbative problem with the Momentum Average (MA) analytical approximation [6, 13, 14] and three different numerical techniques: the Diagrammatic Monte Carlo (DMC) [7], the Limited Phonon Basis Exact Diagonalization (LPBED)

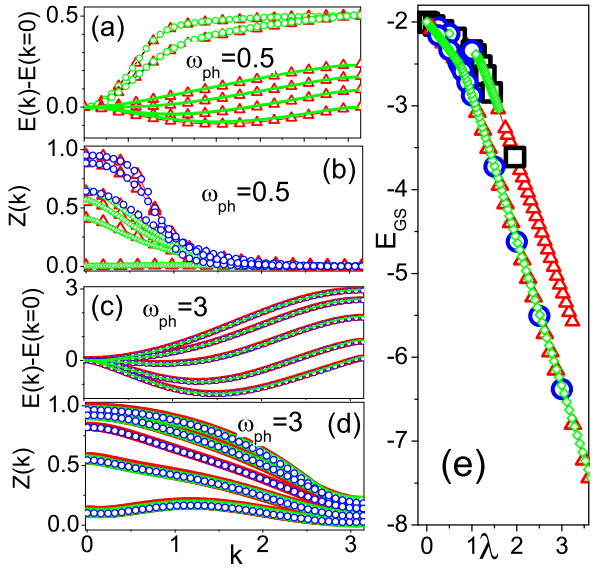

FIG. 1: (Color online) The polaron dispersion relation $E(k) - E(k=0)$ is shown in (a) and (c), and the GS Z-factors $Z(k)$ at momentum k are shown in (b) and (d). Red (blue) triangles (circles) correspond to LPBED (BDMC) methods. In (a), (b), where $\omega_{ph} = 0.5$, $\lambda = 0.25, 0.5, 1.0, 1.094, 1.21, 1.96$ (from top to bottom). In (c), (d), where $\omega_{ph} = 3$, $\lambda = 0.25, 0.5, 1.0, 2.0, 4.0$ (from top to bottom). MA results are shown as green solid curves. In (e) the GS energy for $\omega_{ph} = 0.5$ (upper line) and $\omega_{ph} = 3$ (lower curve) is shown; triangles, rhombi, squares and circles correspond to LPBED, MA, DMC, and BDMC methods, respectively.

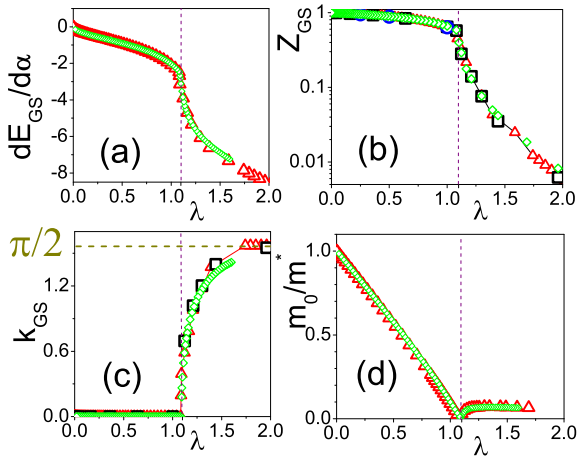

FIG. 2: (Color online) (a) Derivative of the GS energy with respect to α, (b) Z-factor of the GS, (c) wave vector of the GS, and (d) the ratio m_o/m^* of the bare and effective polaronic masses at k_{GS} for $\omega_{ph} = 0.5$ (here $m_o = 1/2t_o$). Red triangles, green rhombi, black squares and blue circles correspond to LPBED, MA, DMC, and BDMC methods, respectively. The vertical dashed arrow indicates the critical coupling λ_c.

[16], and the Bold Diagrammatic Monte Carlo (BDMC) [17] methods. Applications of the first three methods to polaron problems are well documented. However, our implementation of the BDMC method for the SSH model contains several new elements, reviewed in the supporting material.

In the following we display results as functions of λ in both the adiabatic regime (choosing $\omega_{ph} = 0.5$), and the non-adiabatic regime (choosing $\omega_{ph} = 3.0$). We begin with the quasiparticle dispersion $E(k)$ and renormalization factor $Z(k)$ (Figs 1(a)-(d)). One sees immediately that whatever the adiabaticity, the minimum of $E(k)$ is at $k = 0$ for small λ, but at finite k for large λ. At first glance, nevertheless, nothing unusual seems to happen to the ground state energy $E_{GS}(\lambda)$ at the critical value λ_c, where k_{GS} first becomes non-zero (Fig. 1(e)). In fact, the curves in Fig. 1(e) look quite similar to those for Holstein polarons.

However, there is actually a singularity at λ_c. Plots of the dimensionless derivative $dE_{GS}(\lambda)/d\alpha$ (Fig. 2(a)), the overlap $Z_{GS}(\lambda)$ between the ground state at finite λ and the uncoupled ground state (Fig. 2(b)), the momentum $k_{GS}(\lambda)$ for which $E(k)$ is minimized (Fig. 2(c)), and the renormalized effective polaron mass $m^*(\lambda) = (\partial^2 E(\lambda)/\partial k^2)^{-1}|_{k=k_{GS}}$ (Fig. 2(d)), all show a sharp transition at $\lambda = \lambda_c(\omega_{ph})$ (see Fig. 2 for $\omega_{ph} = 0.5$, Fig. 3 for $\omega_{ph} = 3$). At this singularity, the polaronic mass $m^*(\lambda)$ diverges, with corresponding jumps in the first derivatives $dk_{GS}(\lambda)/d\lambda$ and $dZ_{GS}(\lambda)/d\lambda$, and in $d^2E_{GS}(\lambda)/d\lambda^2$. However the average number of phonons $N_{ph}(\lambda)$ in the polaronic polarization cloud does not diverge at λ_c (although it is presumably still singular); $N_{ph}(\lambda_c) < 15$ for all values of the adiabaticity parameter ω_{ph} checked so far. Note also how λ_c varies with ω_{ph} (Fig. 4), initially increasing for small ω_{ph}, but then falling to the asymptotic value $\lambda_c \to 1/2$ in the instantaneous phonon limit $\omega_{ph} \to \infty$. This limit can be derived analytically (see below).

We emphasize here the remarkable agreement obtained between all 4 methods. The three numerical techniques are in principle exact, but all have their practical limitations, such as the sign problem noted below for QMC methods.

(ii) Discussion: The key new feature of couplings $M(k, q)$ like that in Eqs. (2) and (3), compared to k-independent couplings, is that they are non-diagonal in site index. Thus phonons cause the bandwidth to fluctuate, and can by themselves generate hopping between sites. The lowest-order process contributing to E_{GS} is 2nd order in $M(k, q)$; higher corrections come from even powers of M. The same applies to the polaron self-energy, the polaron mass, quasiparticle renormalization, etc. Consider now a pair of vertices, connected by a

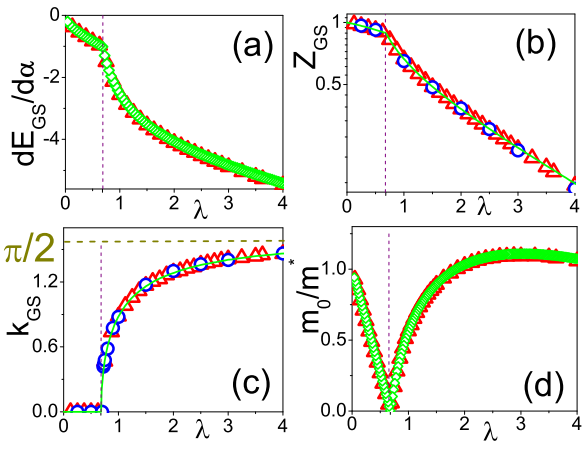

FIG. 3: (Color online) The same as Fig. 2 but for $\omega_{ph} = 3$. MA results in (b), (c) are shown as green solid lines.

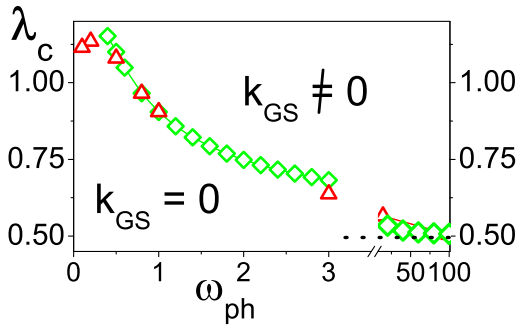

FIG. 4: (Color online) Phase boundary dividing GSs with zero and nonzero momentum. Green squares and red triangles refer to MA and LPBED methods. The horizontal dotted line refers to the instantaneous limit $\lambda_c^{\omega_{ph}\to\infty} = 1/2$.

phonon of momentum q; we have

$$M_{k,-q}M_{k'-q,q} \propto \lambda \sin^2\left(\frac{q}{2}\right) \times \cos\left(k-\frac{q}{2}\right)\cos\left(k'-\frac{q}{2}\right). \quad (4)$$

Three key new features appear in (4):

(a) it can be of either sign when $k \neq k'$. This leads to a 'sign problem' in any Monte Carlo calculation (indeed, for any interaction $M(k,q)$ with non-definite sign); we discuss this in the supporting material. The SSH model is thus representative of a large class of models in which non-diagonal couplings give a sign problem.

(b) multi-site hopping terms involving phonons generate terms in the polaron dispersion of form $E(k) = E_0 - 2t_1^* \cos k - 2t_2^* \cos(2k) - ....$ Now for q-only dependent couplings, the nearest-neighbor hopping $t_1^* \ll t_o$ is exponentially suppressed, and $t_2^* \sim \frac{t_o^2}{\omega_{ph}} e^{-\frac{4\lambda t}{\omega_{ph}}}$ [18] is doubly suppressed, because each requires an intersite polaron cloud overlap. Here, however, an electron can hop from $i-1 \to i \to i+1$, using only V, to first create and then remove a phonon at site i. The associated energy is $t_2^* \propto \Delta t_{i,i+1}\Delta t_{i,i-1}/\omega_{ph}$ where $\Delta t_{i,i-1} \sim \alpha$ is the phonon-induced change in the hopping. Since the phonon-induced displacement $\hat{X}_i$ increases one bond length while decreasing the other, $\Delta t_{i,i+1}\Delta t_{i,i-1} < 0$, ie., $t_2^* \propto -\alpha^2/\omega_{ph}$ is *negative*, favoring a minimum in $E(k) \sim -2t_2^* \cos(2k)$ at $k = \pi/2$, consistent with our results for large λ. This simple analysis indicates how the transition can occur. Of course, higher order terms must also be considered; and a transition like this, signalled by the change in k_{GS}, is certainly not guaranteed for all k-q-dependent couplings (thus the Edwards model in the large λ limit also has a dominant t_2^* term of similar origin; but $t_2^* > 0$, and $k_{GS} = 0$ for all λ [6]).

(c) Finally, consider the limit $\omega_{ph} \to \infty$ for a fixed λ, t_o. The phonon propagator tends to its static limit: $D(q,\omega) = -2\omega_{ph}/(\omega_{ph}^2 - \omega^2) \to \tilde{D} = -2/\omega_{ph}$. The polaron propagator is then dominated by the 2nd-order correction in V, scaling like $\alpha^2/\omega_{ph} \sim \lambda t_o$ (higher order corrections $\sim \alpha^{2n}/\omega_{ph}^{n-1} \sim t_o \lambda^{n-1}\left(\frac{t_o}{\omega_{ph}}\right)^{n-1} \to 0$. Thus, to lowest order in ω_{ph}^{-1} we get from Eq. (4) that

$$\begin{aligned} E(k) &= -2t_o \cos k + \frac{1}{2N^{1/2}}\tilde{D}\sum_q |M(k,q)|^2 \\ &= -2t_o \cos k - \frac{2\lambda t_o}{\sqrt{N}}\sum_q [\sin(k+q) - \sin k]^2 \quad (5) \end{aligned}$$

We see that the dispersion curvature $\left[d^2E(k)/dk^2\right]_{k=0} = 4t_o(1/2-\lambda)$ at $k=0$. Thus, in the large ω_{ph} limit, the effective mass diverges for $\lambda_c(\omega_{ph} \to \infty) = 1/2$. Fig. 4 shows it converges very slowly to this limit.

This discussion shows, at least for sufficiently large ω_{ph}, that there must be a critical coupling strength λ_c at which k_{GS} leaves zero. For small ω_{ph} the existence of a critical point is less clear, because the higher order diagrams can have arbitrary sign; but it is what we find here for all ω_{ph} studied [19]. Note, however, that for $\omega_{ph} < 0.3$, the average number of phonons N_{ph} increases significantly, making numerical simulations very difficult. The MA method is also questionable in this limit.

One is tempted to call this $T = 0$ transition a 'quantum phase transition'. However this is not correct, because any phase transition must involve the cooperative behaviour of an infinite set of degrees of freedom; but here the number of phonons N_{ph} in the polaronic cloud always remains small. Of course with a macroscopic number of polarons in the system, we would see non-analyticity in bulk properties like $dE_{GS}(\lambda)/d\lambda$; but a small number of polarons will be invisible in any thermodynamic property. Thus we simply assert the existence of a non-analyticity, as a function of λ, in the polaronic properties.

We see that polarons having a coupling to a bosonic field depending on both k and q behave in a fundamentally different way from the standard case with only q-dependent coupling. This suggests a large zoology of so far unexplored behavior in many physically relevant systems. Note how surprisingly different the polaronic properties are here. For example, for large λ, $m^*(\lambda)$ *decreases*, and $Z(k_{GS})$ remains quite large. We see that "standard polaronic behavior" is really just a feature of models like the Holstein and Frohlich model.

Experimental signatures of the new behavior - notably, the critical point - will clearly be invisible in any thermodynamic measurements. However the divergence of the effective mass should be easily detectable in transport measurements; the polaron mobility $\mu \sim 1/m^*$ goes to zero at the critical point. Thus in any system where the charge mobility is carried by the polarons, this critical point should be very obvious. It would also be interesting to do ARPES experiments [20], where polarons can be ejected directly from the insulating state, allowing direct measurement of $E(k)$ and $Z(k)$. Apart from polyacetylene, various organic semiconductors are known to have important non-diagonal coupling to phonons [21], as do several dimerized Mott magnetic semiconducting oxides [22]; in some of these, the coupling can be varied somewhat by pressure. However, any quantitative theory for such experiments must also include the coupling to longitudinal phonons, electron-electron interactions, and inter-chain coupling.

(iii) Acknowledgements: We thank G.A. Sawatzky for discussions. NVP acknowledges support from NSF grant (PHY-1005543). NN acknowledges a MEXT Grant-in-Aid for Scientific Research (19048008, 19048015, 21244053). ASM is partly supported by RFBR (10-02-00047a). VC and GDF acknowledge a University of Napoli "Federico II" FARO grant (CUP-E61J10000000003). DM, MB and PCES acknowledge NSERC, CIFAR, FQRNT and PITP for support.

[1] L.D. Landau, Phys. Zh. Sowjet. **3**, 664 (1933); L.D. Landau, S.I. Pekar, Zh. Eksp. Teor. Fiz. **18**, 419 (1948). See also S.I. Pekar, Zh. Eksp. Teor. Fiz. **17**, 1868 (1947); *ibid* **18**, 105 (1948).

[2] H. Frohlich et al, Phil. Mag. **41**, 221 (1950); H. Frohlich, Adv. Phys. **3**, 325 (1954)

[3] S.V. Tyablikov, Zh. Eksp. Teor. Fiz. **23**, 381 (1952); T. Holstein, Adv. Phys. **8**, 343 (1959)

[4] Other examples where polaronic physics is important include magnetism, where one studies spin polarons (see, eg., P. Fazekas, "*Electron Correlation and Magnetism*". World Scientific, 1999), or in biophysics (see, eg., A Scott, Phys. Rep. **217**, 1 (1992).

[5] Early papers in quantum field theory discussing models related to the polaron problem include, eg., T.D. Lee et al, Phys. Rev. **90**, 297 (1953), and S.F. Edwards, R.E. Peierls, Proc. Roy. Soc. A **224**, 24 (1954).

[6] R.P. Feynman, Phys. Rev. **97**, 660 (1955); R.P. Feynman et al, Phys. Rev. **127**, 1004 (1962)

[7] N.V. Prokof'ev and B.V. Svistunov, Phys. Rev. Lett. **81** 2514 (1998); A.S. Mishchenko et al, Phys. Rev. B **62** 6317 (2000)

[8] P.E. Kornilovitch, Phys. Rev. Lett. **81**, 5382 (1998); J. Bonča et al, Phys. Rev. B **60** 1633 (1999); L.C. Ku et al, *ibid* **65** 174306 (2002); J.P. Hague et al, *ibid* **73** 054303 (2006); G. De Filippis et al., *ibid* **72**, 14307 (2005).

[9] A.S. Mishchenko et al Phys. Rev. B **66**, 020301 (2002)

[10] A.S. Mishchenko and N. Nagaosa, Phys. Rev. Lett. **86** 4624 (2001)

[11] B. Gerlach and H. Löwen, Rev. Mod. Phys. **63** 63 (1991).

[12] W.P. Su et al, Phys. Rev. Lett. **42**, 1698 (1979); A. Heeger et al, Rev. Mod. Phys. **60**, 781 (1988)

[13] M. Berciu, Phys. Rev. Lett. **97** 036402 (2006)

[14] G.L. Goodvin and M. Berciu, Phys. Rev. B **78** 235120 (2008)

[15] M. Berciu and H. Fehske, Phys. Rev. B **82** 085116 (2010)

[16] G. De Filippis et al, Phys. Rev. B **80** 195104 (2009)

[17] N.V. Prokof'ev and B.V. Svistunov, Phys. Rev. B **77** 125101 (2008).

[18] F. Marsiglio, Physica C **244**, 21 (1995).

[19] Variational calculations support this conclusion; see J. Sun et al., Phys. Rev. B **79**, 155112 (2009)

[20] A. Damascelli et al, Rev. Mod. Phys. **75**, 473 (2003)

[21] A. Troisi, G. Orlandi, Phys. Rev. Lett. **96**, 086601 (2006); H. Ding et al., Appl. Phys Lett. **96**, 222106 (2010); S.F. Nelson et al., Appl. Phys. Lett. **72**, 1854 (1998).

[22] S.J. Pearton et al., Semicond. Sci. Tech. **19**, R59 (2004).

SUPPORTING MATERIAL

(i) Quantum Monte Carlo Methods: As discussed in the main text, a key feature of the problem addressed here is that any Quantum Monte Carlo (QMC) method is faced by a sign problem (whereas in the conventional polaron problem, with q-dependent coupling only, the imaginary time polaron Green's function and self-energy are sign-definite). Since the sign change can only happen when the internal particle line changes momentum, we see that non-crossing diagrams are positive-definite and only a fraction of the crossing diagrams will have an overall negative sign. This is of course not as severe as the sign-alternating series found in the many-body fermionic case.

The Bold Diagrammatic Monte Carlo (BDMC) technique [1] is a sign-problem tolerant method for many-body problems. It is thus a natural fit to the SSH polaron, and is one of the four techniques used in this letter. It improves on the simpler Green's Function Diagrammatic Monte Carlo[2] (G-DMC)and Self-Energy Monte Carlo (Σ-DMC) methods. The former is a Monte Carlo sampling of the conventional Feynman diagram expansion for the Green's function $G(k, \tau)$ where k and τ are the momentum and imaginary time respectively. The Σ-DMC method also expands the self-energy $\Sigma(k, \tau)$ diagrammatically, but contains fewer terms, thus provid-

ing faster convergence. The BDMC method further reduces the number of diagrams to be sampled by self-consistently renormalizing the particle propagator, and using this to draw subsequent diagrams. By repeated iteration of this procedure, the number of diagrams accounted for by the BDMC method, grows exponentially with simulation time, instead of linearly as in other QMC methods.

In both Σ-DMC and BDMC the renormalized propagator $G'(k,\,\tau)$ is obtained by solving Dyson's equation in imaginary frequency ξ using a FFT algorithm to convert between τ- and ξ-dependent quantities. Normalization of $\Sigma(k,\,\tau)$ is enforced using $\lim_{\tau\to 0}\Sigma(k,\,\tau) = \lambda\omega t[2-\cos(2k)]$. Quantities such as the polaron dispersion, quasiparticle weight and effective mass can all be obtained either from $\Sigma(k,\,\tau)$ or $G(k,\,\tau)$. Fig. 5 compares the diagrammatic formulation of the various QMC methods.

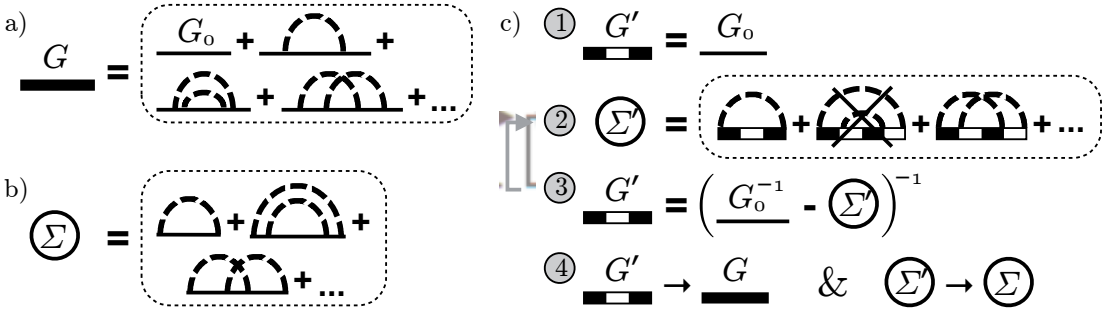

FIG. 5: Comparison between the (a) G-DMC, (b) Σ-DMC and (c) BDMC methods. Dashed-lined boxes represent MC sampling of the appropriate diagram expansion. Some extra restrictions apply in the case of BDMC to avoid double counting. Step 2 and 3 of BDMC are repeated until desired convergence. Step 3 consists in solving Dyson's equation in imaginary frequency.

(ii) The Momentum Average Method: The Momentum Average (MA) approximation solves the equation of motion for the Green's function $G(k,\omega) = \langle 0|c_k(\omega + i\eta - \mathcal{H})^{-1}c_k^\dagger|0\rangle$, where $|0\rangle$ is the vacuum. As usual, this solution appears in the form of an infinite hierarchy of coupled equations of motion. The main idea behind MA is to simplify the coefficients multiplying the generalized Green's function in these equations so that this infinite hierarchy can be solved (quasi)analytically. Because it is formulated in terms of equations of motion and because there is no truncation at any order, MA is a non-perturbative approximation. In diagrammatic terms, MA is equivalent [3] to a sum of all diagrams for the self-energy expansion, after discarding exponentially small contributions (compared to what is kept) from each diagram. As a result, MA satisfies multiple spectral weight sum rules exactly.

The guidance on how to approximate the equations of motions (which also determines what parts of the diagrams are discarded) comes from the variational meaning of MA. Essentially, one makes some assumption about the nature of the bosonic cloud, and keeps only terms consistent with it [3–5]. For the Holstein model, it is already a very good approximation to assume that all the bosons in the cloud are at the same site – however, there can be arbitrarily many such bosons, and the particle can be arbitrarily far from the cloud. Further systematic increases in the variational space lead to systematic improvements of the MA approximation [3]. For more complicated models, one needs to allow the cloud to be more extended. In this work, we use the straightforward generalization to our "SSH model" of the 3-site version of MA detailed for the Edwards model in Ref. [6].

(iii) The Limited Phonon Basis Exact Diagonalization method: The Limited Phonon Basis Exact Diagonalization (LPBED) method[7] is based on the standard Lanczos algorithm. It uses the translational symmetry associated with periodic boundary conditions, requiring that the states have a definite momentum (the Hamiltonian is block diagonalized). Each basis vector is a linear superposition with appropriate phases of the translational copies (charge carrier and lattice configurations are together rigidly translated) of a state having the electron fixed at a site and phonon quanta located around it. The real bottleneck comes from the Hilbert space required by the phonon basis, which is unlimited even in a finite size lattice. To circumvent this difficulty, LPBED takes into account only a finite number of phonon states. The states are chosen starting from the observation[4] that the MA approximation within the Holstein model can be recovered by using a restricted basis where all the bosons in the cloud are at the same site and arbitrarily far from the electron. In the SSH model, where the coupling charge-lattice is not local and is related to the hopping,

the phonon cloud has to be more extended to describe in an appropriate way the relevant physical processes (the extension increases as ω_{ph} decreases). In this work we use a cluster of 5 neighbouring sites (the cluster can be arbitrarily far from the electron). Moreover we include an additional pair of phonons located on any pair of lattice sites. In this way the scattering processes between the charge carrier and up to two phonons in q-space are exactly treated, so that the weak coupling limit is optimally described. The main advantage of the LPBED method is that it is possible to calculate not only the self energy of the quasiparticle but any correlation function.

[1] N.V. Prokof'ev and B.V. Svistunov, Phys. Rev. B 77, 125101 (2008).

[2] N.V. Prokof'ev and B.V. Svistunov, Phys. Rev. Lett. 81, 2514 (1998).

[3] M. Berciu and G. L. Goodvin, Phys. Rev. B **76**, 165109 (2007)

[4] O. S. Barisic, Phys. Rev. Lett. **98**, 209701 (2007)

[5] M. Berciu, Phys. Rev. Lett. **98**, 209702 (2007)

[6] M. Berciu and H. Fehske, Phys. Rev. B **82**, 085116 (2010)

[7] G. De Filippis, V. Cataudella, A. S. Mishchenko, C. A. Perroni, and N. Nagaosa, Phys. Rev. B **80**, 195104 (2009).